

# FABRICATION OF TiO<sub>2</sub>/DYE-SENSITIZED SOLAR CELLS (DSCs) USING DYE EXTRACTS AND THEIR MIXTURE AS PHOTSENSITIZERS

## Authors' contributions

This work was carried out in collaboration between all authors. Authors TOA, POA and NA designed the study. Author TOA wrote the protocol and wrote the first draft while, authors NA and AAL carried out the experimental work and analyses. Authors TOA and AAL managed the literature searches. All authors read and approved the final manuscript.

## Original Research Article

### ABSTRACT

In this work we have reported an investigation on *Hibiscus sabdariffa* and *Delonix regia* dye extracts and their mixture as natural sensitizers for TiO<sub>2</sub>/DSCs. A shift in the absorption maximum toward the lower energy of the ultraviolet-visible spectrum was observed for the dye mixture and a shift in the absorption maximum towards the higher energy of the ultraviolet-visible spectrum was observed for the dye extracts. The optical band gaps obtained at the point where the absorption spectra showed strong cut offs range from 1.79eV to 2.40eV. Also, we have used TiO<sub>2</sub> thin films of thickness 5.2μm and the Light Harvesting Efficiencies (LHE) of the dye extracts and the dye mixture adsorbed onto TiO<sub>2</sub> surface were close to unity. The average diameter of the TiO<sub>2</sub> films obtained from SEM is in the range of 25-40nm reflecting that the TiO<sub>2</sub> films are transparent and suitable for DSC application. The XRD pattern revealed the TiO<sub>2</sub> films to be of anatase form and the structure type is tetragonal with 3.53217Å as the *d-spacing* for the most prominent peak,  $2\theta=25.2139^\circ$  (ICDD data file: 01-075-8897). Three (3) DSCs each of 0.52 cm<sup>2</sup> active area were assembled and subjected to current-voltage characterization using a standard overhead Veeco viewpoint solar simulator equipped with AM 1.5 filter to give a solar radiation of 1000 W/m<sup>2</sup> and coupled to Keithley source meter (model 4200SCS). The photoelectrochemical performance of the fabricated DSCs showed open-circuit voltages ( $V_{oc}$ ) varied from 0.42 to 0.53 V, the short-circuit current densities ( $J_{sc}$ ) ranged from 0.10mAcm<sup>-2</sup> to 0.90mAcm<sup>-2</sup> and the fill factors ( $FF$ ) varied from 12 to 38%. The best overall solar power conversion efficiency of 0.13% was obtained, under AM 1.5 irradiation and a maximum short circuit current density of 0.90mAcm<sup>-2</sup>. Nevertheless, pure *Hibiscus sabdariffa* and *Delonix regia* dye extracts proved to be rather poor sensitizers as can be seen by the low spectra absorption at lower energies with current densities of 0.17mAcm<sup>-2</sup> and 0.10mAcm<sup>-2</sup> respectively. The solar power conversion efficiencies for *Hibiscus sabdariffa* and *Delonix regia* dye extracts were 0.01% and 0.02% respectively. In our earlier studies, we highlighted an established fact that raw natural dye mixtures exhibit better performance than pure dye extracts. Thus, the power conversion efficiency of 0.13% observed for the dye mixture sensitized TiO<sub>2</sub>/DSC corresponds to an increment in the neighborhood of 85% to 92% over the pure dye extracts sensitized TiO<sub>2</sub>/DSCs.

Keywords: Natural dyes, dye mixture, light harvesting efficiency, molar extinction coefficient, TiO<sub>2</sub>-DSC, optical band gap, power conversion efficiency.

## 40 1.0 INTRODUCTION

41 The power conversion efficiencies of natural dye-sensitized solar cells are low compared to solar  
42 cells sensitized with inorganic and synthetic dyes [1, 2, 3]. This is due to weak bonding between  
43 the natural dyes and TiO<sub>2</sub> surface which ultimately leads to low short circuit current density  
44 deliverable by the solar cells [4]. Other reasons include transformation of the natural dye  
45 functional groups from a more stable state (flavilium state) to an unstable state (quinoidal state)  
46 upon attachment to the TiO<sub>2</sub> surface which is as a result of high pH values [5, 6, 7]. This unstable  
47 state is usually characterized by long bond length functional groups that prevent dye molecules  
48 from arraying effectively on the TiO<sub>2</sub> film thereby causing low electron transfer from the dye  
49 molecules to the conduction band of TiO<sub>2</sub>. Finally, the masking and agglomeration effects of  
50 natural dyes which limit the light harvesting efficiency to ultraviolet and the onset of the visible  
51 light spectrum [5, 7, 8, 9, 10].

52  
53 Several research efforts have been made to improve the interaction between the natural dyes and  
54 TiO<sub>2</sub> surface in order to achieve high power conversion efficiency. These include the use of  
55 appropriate extraction solvents, synergistic effect of dyes derived from single species such as  
56 algal derived photosynthetic pigments, organic acids and mixed dyes [11, 12, 13, 14, 15, 16, 17,  
57 18, 19]. Thus, it was established that mixed dye system would account for many possible types  
58 of interactions between dyes with various constituents present, but this is yet to be thoroughly  
59 understood [20]. Although, there could be more possible ways to increase the efficiency of solar  
60 cells sensitized with natural pigments but it is evident from the equation for power conversion  
61 efficiency [equation (1) below] that high values of short circuit current density ( $J_{sc}$ ), open  
62 circuit voltage ( $V_{oc}$ ) and fill factor ( $FF$ ) lead to high efficiency in any solar cell. As such, it is  
63 necessary to improve these three parameters in order to raise power conversion efficiency of a  
64 DSC.

65  
66 In our previous studies, we developed and characterized DSC based on TiO<sub>2</sub> nanoparticles  
67 coated with Hibiscus sabdariffa (Zobo) and the overall solar power conversion efficiency of  
68 0.033% and a maximum current density of 0.17mAcm<sup>-2</sup> were obtained [21]. Typically, low peak  
69 absorption coefficient, small spectra width and very low power conversion efficiency of this  
70 DSC boosted additional studies oriented; on one hand, to the use of a new natural sensitizer  
71 (Delonix regia) in addition to Hibiscus sabdariffa and their mixture as a promising strategy for  
72 harvesting more light in the higher wavelengths. On the other hand, we hope to increase the  
73 extent of Light Harvesting Efficiency (LHE) within the TiO<sub>2</sub> electrode by depositing a blocking  
74 layer sequentially to enhance the surface area of TiO<sub>2</sub>, to favor cluster formation in TiO<sub>2</sub> nanoparticles  
75 for effective anchorage of the natural dye extracts and their mixture and to improve interconnectivity  
76 among TiO<sub>2</sub> nanoparticles for enhancement in the short circuit current density. Sequel to this, three (3)  
77 DSCs each of 0.52 cm<sup>2</sup> active area were assembled by sandwiching a surlyn polymer foil of 25  
78 μm thickness, as spacer between the photoelectrode and the platinum counter electrode and  
79 characterized using a standard overhead Veeco viewpoint solar simulator equipped with AM 1.5  
80 filter to give a solar radiation of 1000 W/m<sup>2</sup> and coupled to a Keithley source meter (model  
81 4200SCS) which was connected to the computer via GPIB interface for data acquisition.

82  
83  
84  
85

## 86 2. MATERIALS AND METHODS

87 Titanium isopropoxide, Titanium nanoxide, acetylacetonate, ethanol, isopropanol, fluorine doped  
88 tin-oxide (FTO) conducting glass [ $11.40\text{ ohm/m}^2$ ,  $(1.00 \times 1.00)\text{cm}^2$ ], electrolyte (iodolyte-AN-  
89 50), sealing gasket (surlyn-SX1170-25PF), and screen-printable platinum catalyst, (Pt-catalyst  
90 T/SP) all were obtained from SOLARONIX. Dye extracts were obtained from the natural  
91 products (*Hibiscus sabdariffa* and *Delonix regia*). A mixture of 0.3M of titanium isopropoxide,  
92 1.2M acetylacetonate and isopropanol was spin coated three (3) times with different  
93 concentrations sequentially as blocking layer on the pre-cleaned fluorine doped tin-oxide (FTO)  
94 conducting glasses and sintered at  $150^\circ\text{C}$  for four minutes each time the deposition was made.  
95 Subsequently, a paste of titanium nanoxide in propanol in the ratio 1:3 was screen printed on the  
96 three (3) fluorine doped tin-oxide (FTO) conducting glasses and allowed to dry at  $125^\circ\text{C}$  in open  
97 air for 6 minutes.

98 The FTO/TiO<sub>2</sub> glass electrodes were sintered in a furnace at  $450^\circ\text{C}$  for 40 minutes and allowed  
99 to cool to room temperature to melt together the TiO<sub>2</sub> nanoparticles and to ensure good  
100 mechanical cohesion on the glass surface. Dried leaves of *Hibiscus sabdariffa* and *Delonix regia*  
101 were crushed into tiny bits and boiled in 75ml of deionized water for 15 minutes. The residue  
102 was removed by filtration and the resulting extracts were centrifuged to further remove any solid  
103 residue while a mixture in the ratio 50:50 by volume of the dye extracts was made. The dye  
104 extracts and the mixture were used directly as prepared for the construction of the DSCs at room  
105 temperature. A scattering layer of TiO<sub>2</sub> was also deposited on the TiO<sub>2</sub> electrodes before the  
106 electrodes were immersed (face-up) in the natural dye extracts and their mixture for 18h at room  
107 temperature for complete sensitizer uptake. This turned the TiO<sub>2</sub> film from pale white to  
108 sensitizer colour. The excess dye was washed away with anhydrous ethanol and dried in  
109 moisture free air.

110 The thickness of TiO<sub>2</sub> electrodes and the deposited scattering layers was determined using  
111 Dekker Profilometer. Surface morphology of the screen-printed TiO<sub>2</sub> nanoparticles was observed  
112 using EVOI MA10 (ZEISS) multipurpose scanning electron microscope operating at  $20\text{kV}$   
113 employing secondary electron signals while the corresponding Energy Dispersive Spectra (EDS)  
114 were obtained using characteristic x-rays emitted by TiO<sub>2</sub> nanoparticles. The X-ray diffraction  
115 (XRD) pattern of the screen-printed TiO<sub>2</sub> nanoparticles at room temperature was recorded using  
116 X-ray Diffractometer; Panalytical Xpert-Pro,  $PW3050/60$ , operating at  $30\text{mA}$  and  $40\text{kV}$ , with  
117 monochromatic  $\text{Cu-K}\alpha$  radiation, of wavelength  $\lambda = 1.54060\text{\AA}$ . A scanned range  $3-80.00553^\circ 2\theta$ ,  
118 with a step width of  $0.001^\circ$  was used. The pattern was analyzed and the peaks were identified  
119 using ICDD data file (01-075-8897). The UV-Visible ( $UV\text{-}Vis$ ) absorption measurements of the  
120 dye extracts, their mixture and the dye extracts and their mixture on the screen printed TiO<sub>2</sub>  
121 electrodes were carried out with *Avante UV-VIS* spectrophotometer (model-LD80K). From these  
122 measurements, plots for the absorbance, Light Harvesting Efficiency ( $LHE$ ) and molar extinction  
123 coefficient versus the wavelengths of interest were obtained using the relevant expressions from  
124 [4].

125 Three (3) DSCs each of  $0.52\text{cm}^2$  active area were assembled by sandwiching a surlyn polymer  
126 foil of  $25\mu\text{m}$  thickness, as spacer between the photoelectrode and the platinum counter electrode  
127 and then hot-pressed at  $80^\circ\text{C}$  for  $15\text{s}$ . A drop of liquid electrolyte was introduced into the cell  
128 assemblies via pre-drilled holes on the counter-electrodes and sealed using amosil sealant. In

129 order to have good electrical contacts, a strip of wire was attached to both sides of the FTO  
130 electrodes. Finally, the DSCs were subjected to current-voltage characterization using a standard  
131 overhead Veeco viewpoint solar simulator equipped with *Air Mass 1.5* (AM 1.5) filter to give a  
132 solar radiation of  $1000 \text{ W/m}^2$  and coupled to *Keithley* source meter (model 4200SCS) which was  
133 connected to the computer via  *GPIB* interface for data acquisition. Subsequently, the working  
134 electrode and counter electrode of the DSC were connected in turn to the positive and negative  
135 terminals of the digital *Keithley* source meter respectively. The bias was from short circuit to  
136 open circuit and was obtained automatically using LabVIEW software from National  
137 Instruments Inc, USA. From the data, *I-V* curves were plotted in real time for the DSCs under  
138 illuminated condition. Following this, the photovoltaic parameters viz; the open circuit voltage  
139 ( $V_{oc}$ ) and short circuit current ( $I_{sc}$ ) were obtained from the *I-V* curves for the cells. The fill factor  
140 (*FF*) and the power conversion efficiency for the cells were obtained using the following  
141 relations:

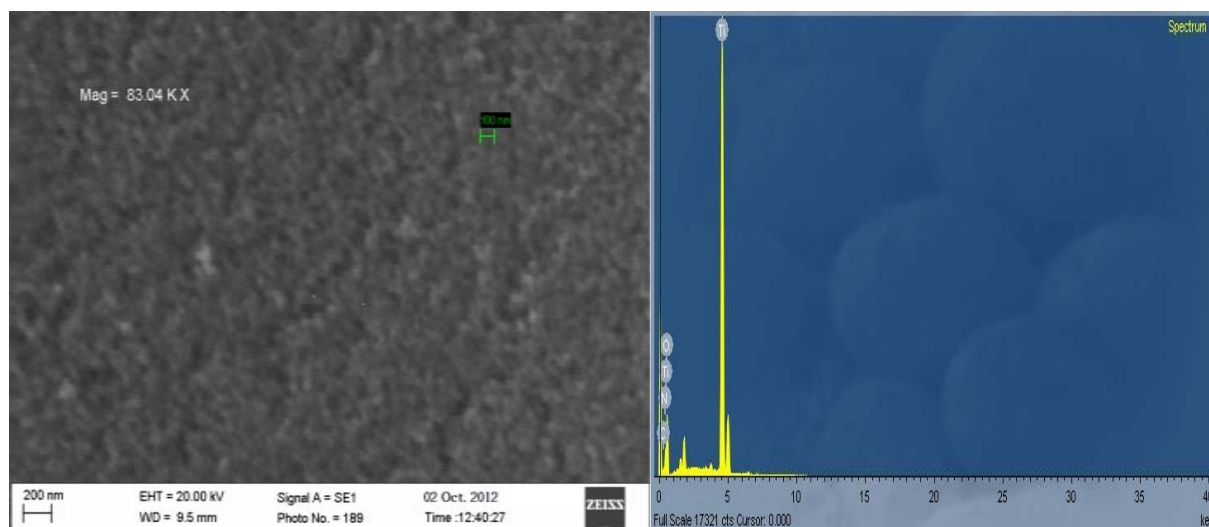
$$142 \quad FF = \frac{P_m}{V_{oc} \cdot I_{sc}} \quad \text{and} \quad \eta = \frac{FF \cdot V_{oc} \cdot J_{sc}}{I_{in}} \quad (1)$$

143  
144  
145  
146

### 3.0 RESULTS AND DISCUSSION

147 The image presented in Figure 1 obtained using characteristic x-rays emitted by  $\text{TiO}_2$   
148 nanoparticles was observed at a magnification of 83.04kX. The uniform contrast in the image  
149 revealed  $\text{TiO}_2$  to be practically isomorphous with titanium and oxygen being the dominant  
150 elements with concentration of about 99.9% as depicted in the EDS spectra (Figure 1b). The  
151 morphology of  $\text{TiO}_2$  nanoparticles is such that the particles are closely packed and spherical in  
152 shape. The average diameter of the particles is in the range of 25-40nm reflecting that  $\text{TiO}_2$   
153 nanoparticles are transparent and suitable for DSC application. The thickness of  $\text{TiO}_2$  on the  
154 FTO conducting glass determined using Dekker Profilometer was found to be  $5.2 \mu\text{m}$  for each  
155 photoelectrode and that of the deposited scattering layers was found to be  $1 \mu\text{m}$ . The XRD  
156 pattern revealed the compound name for the  $\text{TiO}_2$  electrode to be anatase syn., and the structure  
157 type is tetragonal with  $3.53217 \text{ \AA}$  as the *d-spacing* for the most prominent peak,  $2\theta = 25.2139^\circ$   
158 (ICDD data file: 01-075-8897). Other prominent peaks occur at  $2\theta = 37.7883^\circ, 48.0463^\circ,$   
159  $53.9110^\circ, 55.0481^\circ, 62.7104^\circ$  and  $75.1376^\circ$  with *d-spacing*  $d = 2.38075 \text{ \AA}, 1.89370 \text{ \AA}, 1.70073 \text{ \AA},$   
160  $1.66826 \text{ \AA}, 1.48160 \text{ \AA}$  and  $1.26338 \text{ \AA}$ .

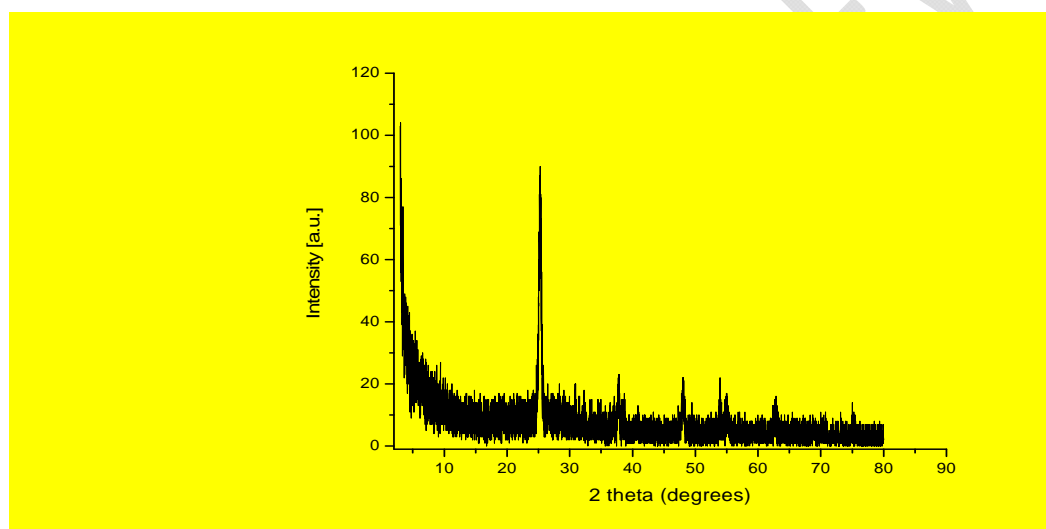
161  
162 In figure 2, the dye extracts and their mixture exhibit absorption maxima slightly above  $400 \text{ nm}$   
163 and the most prominent shoulders occur slightly above  $500 \text{ nm}$ . But upon sensitization on  $\text{TiO}_2$ ,  
164 there was reduction in absorption maxima and the prominent shoulders for the dye extracts while  
165 an enhancement in the absorption maximum with a shift toward high wavelengths ( $450 \text{ nm} -$   
166  $600 \text{ nm}$ ) was observed for the dye mixture and the prominent shoulder broadened toward the  
167 higher wavelengths ( $750 \text{ nm} - 900 \text{ nm}$ ) with reduced absorption intensity for the mixture.  
168



169  
170  
171  
172

(a)

(b)



173  
174  
175  
176  
177  
178

(c)

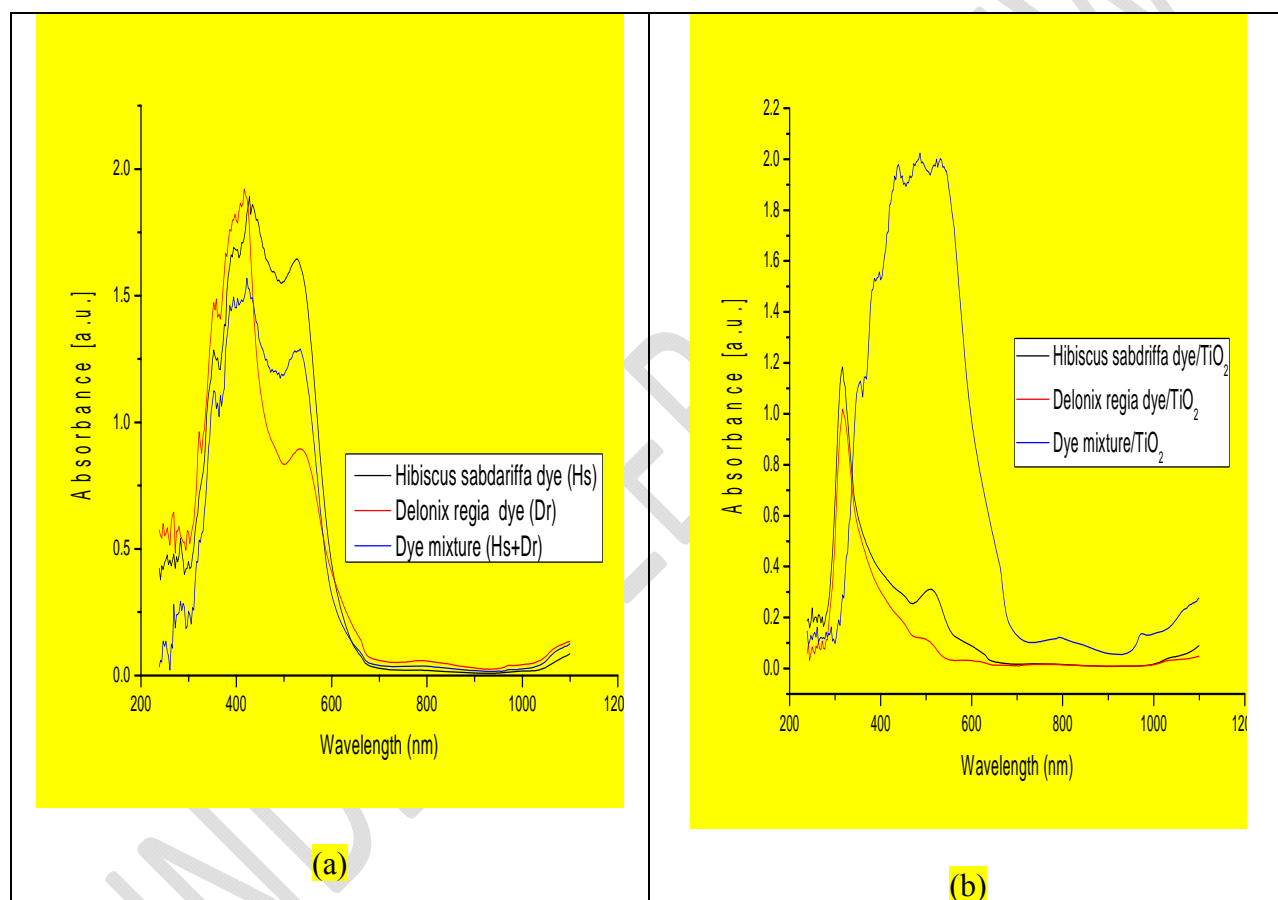
Figure 1:  $\text{TiO}_2$  structural characteristics: (a) Surface morphology, (b) Energy Dispersive Spectra and (c) XRD pattern for the screen printed  $\text{TiO}_2$ .

179 Chemisorption of anthocyanins on  $\text{TiO}_2$  was been reported by [22] to be as a result of alcoholic  
180 bound protons which condense with the hydroxyl groups present at the surface of nanostructured  
181  $\text{TiO}_2$ . Such attachment to the  $\text{TiO}_2$  surface stabilizes the excited state, thus shifting the absorption  
182 maximum towards the lower energy of the spectrum. In our study, a shift in the absorption  
183 maximum towards the lower energy of the spectrum was observed for the dye mixture adsorbed  
184 on  $\text{TiO}_2$  and a shift in the absorption maximum towards the higher energy of the spectrum was  
185 observed for the dye extracts adsorbed on  $\text{TiO}_2$ . This observation suggests that there was  
186 effective adsorption of the dye mixture onto  $\text{TiO}_2$  surface which could be attributed to the low  
187  $pH$  value and the short bond length of the  $\text{OH}$  groups present in the dye mixture. These  $\text{OH}$

188 groups favour the formation a strong bond with the oxide surface and also good arraying to the  
189  $TiO_2$  film effectively. The shift may also be attributed to the changing of the anthocyanin  
190 molecule from the unstable quinoidal state to the more stable flavilium state to upon chelation.

191 It is an established fact that the light absorption by a dye monolayer is small since the cross  
192 section for photon absorption of most photosensitizers is much smaller than the geometric area  
193 occupied on the semiconductor surface, but with thin film semiconductor the obtainable LHE is  
194 usually close to unity [23]. In this work, we have used  $TiO_2$  thin film of thickness  $5.2\mu m$  and the  
195 LHE of the dye extracts and the dye mixture adsorbed onto  $TiO_2$  surface is close to unity.

196



197

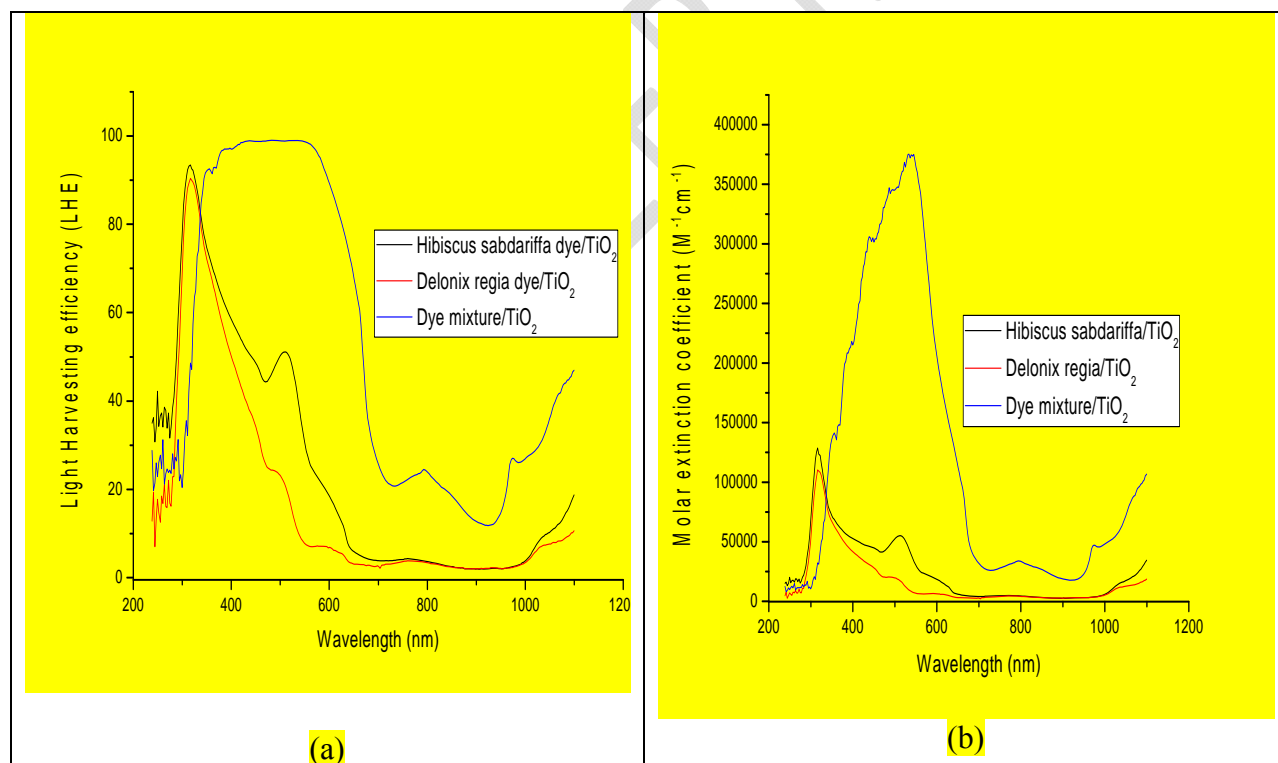
198 **Figure 2: UV–VIS absorption spectra for (a) Hibiscus sabdariffa dye extract, Delonix regia dye**  
199 **extract and Mixture of dye extracts and (b) Hibiscus sabdariffa /  $TiO_2$ , Delonix regia/ $TiO_2$  and**  
200 **Mixture of dye extracts/ $TiO_2$ .**

201

202 The light harvesting efficiency values obtained are plotted against wavelengths as shown in  
203 figure 3. The absorption band of the dye extracts after sensitization on  $TiO_2$  becomes a bit  
204 discrete after sensitization but quite broad for the dye mixture after sensitization. Whilst the  
205 molar extinction coefficients are very high for the dye extracts and the mixture, it turned out that

206 only small areas are being covered by the solar irradiance spectrum for the dye extracts but an  
207 increase in the area was observed for the dye mixture. Most notably, the spectra bandwidth is  
208 within the range of  $150\text{nm}$  to  $200\text{nm}$  for the dye extracts but an increase in the vicinity of  $400\text{nm}$   
209 to  $500\text{nm}$  was observed for the dye mixture. This increase in the spectra bandwidth significantly  
210 enhances the photocurrent density for the dye mixture/ $\text{TiO}_2$ -DSC as evident from current-voltage  
211 characterization.

212 Current density and power versus voltage characteristics of the DSCs are plotted and shown in  
213 figure 4. The photovoltaic parameters are determined and tabulated in Table 1. The current  
214 density ranges from  $0.17\text{mAcm}^{-2}$  to  $0.90\text{mAcm}^{-2}$ , the open circuit voltage ranges from  $0.42\text{V}$  to  
215  $0.53\text{V}$ , the fill factor from 12% to 38% and the power conversion efficiency ranges from 0.01%  
216 to 0.13%. Thus, it is evident from table 1 that high values of  $J_{sc}$ , and  $V_{oc}$  are responsible for the  
217 higher efficiency obtained for the dye mixture/ $\text{TiO}_2$ -DSC compared to those of the parent dyes.  
218 In our previous studies, we developed and characterized DSC based on  $\text{TiO}_2$  nanoparticles  
219 coated with Hibiscus sabdariffa (Zobo) and the overall solar power conversion efficiency of  
220 0.033% and a maximum current density of  $0.17\text{mAcm}^{-2}$  were obtained [21]. This boosted  
221 additional studies oriented to the use of dye mixture (Hibiscus sabdariffa plus delonix regia)  
222 leading to an enhancement in the light harvesting efficiency and hence the photocurrent density  
223 which is owed to the high peak absorption coefficient and large spectra bandwidth.  
224  
225



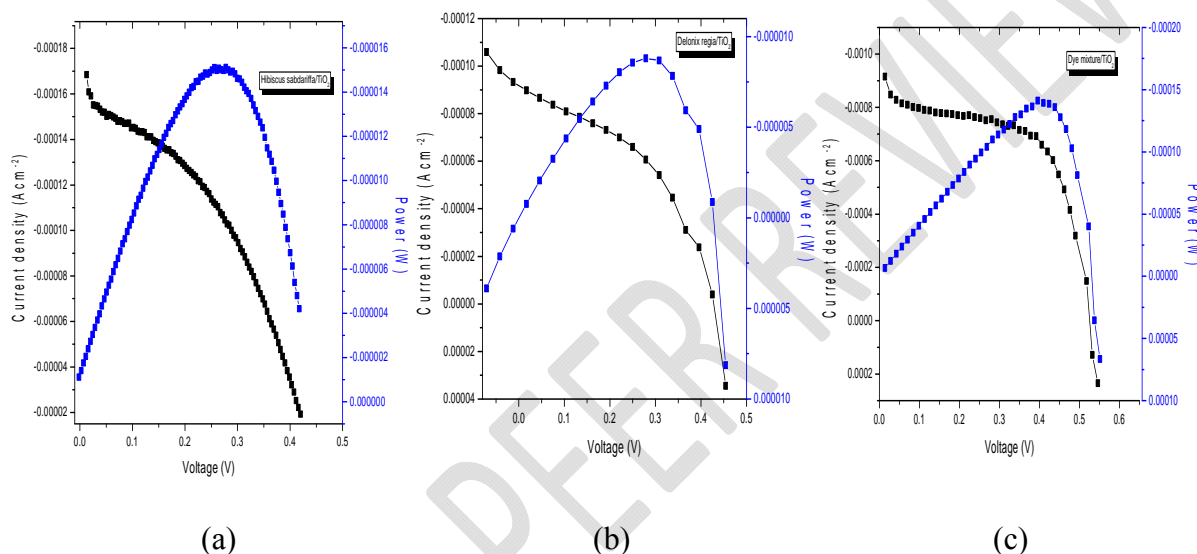
226  
227  
228 **Figure 3: Light Harvesting Efficiency (LHE) for (a) Hibiscus sabdariffa /  $\text{TiO}_2$ , Delonix**  
229 **regia/ $\text{TiO}_2$  and Mixture of dye extracts/ $\text{TiO}_2$  and (b) Hibiscus sabdariffa /  $\text{TiO}_2$ , Delonix**  
230 **regia/ $\text{TiO}_2$  and Mixture of dye extracts/ $\text{TiO}_2$ .**



231 **Table 1: Photovoltaic parameters of the DSCs sensitized with *Hibiscus sabdariffa* dye,**  
 232 ***Delonix regia* dye and their mixture**

DSC	$J_{sc}(mAcm^{-2})$	$V_{oc}(V)$	FF	$\eta$ (%)
<i>H. sabdariffa</i> /TiO <sub>2</sub>	0.17	0.42	0.12	0.01
<i>Delonix regia</i> /TiO <sub>2</sub>	0.10	0.45	0.38	0.02
Dye mixture /TiO <sub>2</sub>	0.90	0.53	0.28	0.13

233



234

235

236 Figure 4: Current density and Power versus voltage for (a) TiO<sub>2</sub>-DSC sensitized with *Hibiscus*  
 237 *sabdariffa* dye, (b) TiO<sub>2</sub>-DSC sensitized with *Delonix regia* dye and (c) TiO<sub>2</sub>-DSC sensitized  
 238 with dye mixture.

239

240 In this work, it was discovered that *TiO<sub>2</sub>* band gap was reduced upon sensitization with the  
 241 extracted dyes and their mixture. The optical band gaps were obtained at the point where the  
 242 absorption spectra showed a strong cut off, when the absorbance values are minimum. The  
 243 values range from  $1.79eV$  to  $2.40eV$ . The band shifts could be attributed to molecular transitions  
 244 that take place when the dye molecules chelate with *TiO<sub>2</sub>*. Typically, anthocyanin dyes exhibit  $\pi$   
 245 -  $\pi^*$  orbital transition which is attributed to the wavelength range between  $500nm$  to slightly  
 246 above  $650nm$ . In this work, the cut off wavelength for the spectra ranges between  $600nm$  to  
 247 slightly above  $700nm$ . Finally, it is well known that proton adsorption causes a positive shift of  
 248 the Fermi level of the *TiO<sub>2</sub>*, thus limiting the maximum photovoltage that could be delivered by  
 249 the cells [22]. Nevertheless, the dye mixture proved to be a better sensitizer compared to pure  
 250 *Hibiscus sabdariffa* and *Delonix regia* that exhibited low spectral absorption at lower energies.  
 251 However, no deviation from this trend was observed when the duration of continuous stimulated  
 252 sunlight illumination was increased for several hours.



#### 253 4.0 CONCLUSION

254 In this work we have reported an investigation on *Hibiscus sabdariffa* and *Delonix regia* dye  
255 extracts and their mixture as natural sensitizers of  $TiO_2/DSCs$ . The best overall solar power  
256 conversion efficiency of 0.13% was obtained, under AM 1.5 irradiation and a maximum current  
257 density of  $0.90mAcm^{-2}$ . Nevertheless, pure *Hibiscus sabdariffa* and *Delonix regia dye extracts*  
258 proved to be rather poor sensitizers as can be seen by the low spectral absorption at lower  
259 energies with current density of  $0.17mAcm^{-2}$  and  $0.10mAcm^{-2}$  respectively. The solar power  
260 conversion efficiency for *Hibiscus sabdariffa* and *Delonix regia* dye extracts are 0.01% and  
261 0.02% respectively. In our earlier studies, we highlighted an established fact that raw natural dye  
262 mixtures exhibit better performance than pure dye extracts. Thus, the power conversion  
263 efficiency of 0.13% observed for the dye mixture corresponds to 92% and 85% increment over  
264 the pure dye extracts sensitized  $TiO_2/DSCs$ . This could be related to the specific pools of  
265 ancillary molecules present in the dye mixture of (*i.e.*, alcohols, organic acids, *etc.*) which act as  
266 coadsorbates, suppressing recombination with the electrolyte, reducing dye aggregation and  
267 favouring charge injection. Although the efficiencies obtained with this natural dye extracts and  
268 the dye mixture are still below the current requirement for large scale practical application, the  
269 results are encouraging and may boost additional studies focused on the modification of solar  
270 cell components compatible with the dye mixture. In view of this, we are currently exploring the  
271 possibility of increasing the power-conversion efficiency of the  $DSCs$  based on  $TiO_2$  using  
272 modified  $TiO_2$  and counter electrodes and *Delonix regia*.

273

#### 274 ACKNOWLEDGEMENTS

275 We thank Physics Advanced Laboratory, Sheda Science and Technology Complex, FCT,  
276 Abuja, Nigeria for technical assistance during the experimental characterization.

277

#### 278 COMPETING INTERESTS

279 Authors have declared that no competing interests exist.

280

281

#### 282 REFERENCES

283

284

- 285 1. Calogero G, Di-Marco G, Cazzanti S, Caramori S, Argazzi R, Bignozzi CA. Natural dye  
286 sensitizers for photoelectrochemical cells. *Energ. Environ. Sci.* 2009. 2, Pp.1162– 1172.
- 287 2. Gong J, Liang J, Sumathy K. Review on dye-sensitized solar cells (DSSCs):  
288 fundamental concepts and novel materials. *Renew Sustain Energy Rev.*, 2012. 16(8),  
289 Pp.5848–60.
- 290 3. Nazeeruddin MK, Baranoff E, Grätzel M. Dye-sensitized solar cells: a brief  
291 overview. *Sol Energy*, 2011. 85(6); Pp.1172–8.
- 292 4. Ooyama Y, Harima Y. Photophysical and electrochemical properties, and molecular  
293 structures of organic dyes for dye-sensitized solar cells. *Chem. Phys. Chem.* 2012.  
294 13(18); Pp.4032–80.
- 295 5. Narayan MR, Review: dye sensitized solar cells based on natural photosensitizers.  
296 *Renew Sustain Energy Rev.*, 2012. 16(1); Pp.208–15.
- 297 6. Teoli F, Lucioli S, Nota P, Frattarelli A, Matteocci F, Di Carlo A, Caboni E, Forni C.  
298 Role of pH and pigment concentration for natural dye-sensitized solar cells treated

- 299 with anthocyanin extracts of common fruits. *J Photochem Photobiol A: Chem.*, 2016.  
300 316: Pp. 24–30.
- 301 7. Zhou H, Wu L, Gao Y, Ma T. Dye-sensitized solar cells using 20 natural dyes as  
302 sensitizers. *J. Photochem Photobiol A: Chem.* 2011. 219(2–3); Pp.188–94.
- 303 8. Wongcharee K, Meeyoo V, Chavadej S. Dye-sensitized solar cell using natural dyes  
304 extracted from rosella and blue pea flowers. *Sol. Energy Mater., Sol., Cells.* 2007. 91(7);  
305 Pp.566–71.
- 306 9. Palomares E, Clifford JN, Haque SA, Lutz T, Durrant JR. Control of charge  
307 recombination dynamics in dye sensitized solar cells by the use of conformally  
308 deposited metal oxide blocking layers. *J. Am. Chem. Soc.* 2003.125, Pp. 475–482.
- 309 10. Calogero G, Di-Marco G, Cazzanti S, Caramori S, Argazzi R, Carlo AD, Bignozzi CA.  
310 Efficient dye-sensitized solar cells using red turnip and purple wild Sicilian prickly  
311 pear fruits. *Int J Mol Sci.*, 2010 1(1); Pp.254–67.
- 312 11. Warkoyo W, Saati EA. The solvent effectiveness on extraction process of seaweed  
313 pigment. *Makara Teknol.* 2011. 15(1); Pp.5–8.
- 314 12. Sreekala CO, Jinchu I, Sreelatha KS, Janu Y, Prasad N, Kumar M, Sath AK, Roy MS.  
315 Influence of solvents and surface treatment on photovoltaic response of DSSC based on  
316 natural Curcumin dye. *IEEE J Photovolt.* 2012. 2(3); Pp.312–9.
- 317 13. Shahid M, Shahidul I, Mohammad F. Recent advancements in natural dye applications: a  
318 review. *J Clean Prod.* 2013. 53; Pp. 310–331.
- 319 14. Prima EC, Yuliarto B, Suendo V. Improving photochemical properties of *Ipomea*  
320 *pescaprae*, *Imperata cylindrica* (L.) Beauv, and *Paspalum conjugatum* Berg as  
321 photosensitizers for dye sensitized solar cells. *J Mater Sci: Mater Electron.*, 2014.  
322 25(10); Pp.4603–11.
- 323 15. Damit DNFP, Galappaththi K, Lim A, Petra MI, Ekanayake P. Formulation of water to  
324 ethanol ratio as extraction solvents of *Ixora coccinea* and *Bougainvillea glabra* and  
325 their effect on dye aggregation in relation to DSSC performance. *Ionics.* 2017. 23(2);  
326 Pp.485–95.
- 327 16. Lindley CC, Bjorkman O. Fluorescence quenching in four unicellular algae with  
328 different light harvesting and xanthophyll-cycle pigments. *Photosynth Res.*, 1998. 56(3);  
329 Pp.277–289.
- 330 17. Kumara NTRN, Petrovic M, Peiris DSU, Marie YA, Vijila C, Iskander M,  
331 Chandrakanthi RLN, Lim, CM, Hobley J, Ekanayake P. Efficiency enhancement of  
332 *Ixora* floral dye sensitized solar cell by diminishing the pigments interactions. *Sol*  
333 *Energy.* 2015. 117; Pp.36–45.
- 334 18. Hosseinnzhad M. Improvement performance of dye sensitized solar cells from co-  
335 sensitisation of TiO<sub>2</sub> electrode with organic dyes based on indigo and thioindigo. *Mater*  
336 *Technol.*, 2016. 31(6); Pp.348–51.
- 337 19. Lim A, Damit DNFP., Ekanayake P. Tailoring of extraction solvent of *Ixora coccinea*  
338 flower to enhance charge transport properties in dye-sensitized solar cells. *Ionics.* 2015.  
339 21(10); Pp.2897–904.
- 340 20. Kumara NTRN, Ekanayake P, Lim A, Liew LYC, Iskander M, Ming LC. Layered co-  
341 sensitization for enhancement of conversion efficiency of natural dye sensitized solar  
342 cells. *J Alloy Compd.*, 2013. 581(0); Pp.186–91.

- 343 21. Ahmed TO, Akusu PO, ALU N, Abdullahi MB. Dye-Sensitized Solar Cells based on  
344 TiO<sub>2</sub> Nanoparticles and Hibiscus sabdariffa. British Journal of Applied Science and  
345 Technology (BJAST). 2013. 3(4); Pp.840-846.
- 346 22. Hao S, Wu J, Huang Y. Lin J. Natural dyes as photosensitizers for dye- sensitized  
347 solar cell. Solar Energy. 2006. 80, 209.
- 348 23. Gratzel M. Solar energy conversion by dye-sensitized photovoltaic cells. Inorganic  
349 Chemistry. 2005. 44, 6841.

UNDER PEER REVIEW